Soft Robotics

DOI: 10.1002/ange.201210232

Wavelength-Selective, IR Light-Driven Hinges Based on Liquid Crystalline Elastomer Composites**

*Ryan R. Kohlmeyer and Jian Chen**

Robotics technology has a broad impact on industries as diverse as manufacturing, logistics, medicine, healthcare, military, agriculture, and consumer products. Unlike biological systems, traditional robots have rigid underlying structures that are usually made of metals, which limit their ability to interact with the environment and handle fragile or irregular objects of various shapes and sizes. There has been an increasing interest in the field of bioinspired soft robotics recently.[1–4] With soft materials-based structures and highly redundant degrees of freedom, these robots can be used for carrying soft, fragile payloads without causing damage and working in cluttered and/or unstructured environments by employing large strain deformation.

Liquid crystalline elastomers (LCEs) have fascinated scientists and engineers because they bring together three important features: orientational order exhibited by the mesogenic units in amorphous soft materials, topological constraints owing to cross-links, and responsive molecular shape because of the strong coupling between the orientational order and the mechanical strain. LCEs can translate small molecular movements triggered by an external stimulus into large mechanical motions.[5–12] In contrast to shape-memory polymers, LCEs are shape-changing polymers, which can reversibly switch shapes in response to an external stimulus such as heat, light, or electric field without the need for external mechanical manipulation.[13] LCEs containing photochromic moieties such as azobenzene exhibit reversible bending under alternate irradiation by UV and visible light, owing to a photoinduced change in the molecular orientation of mesogens only in the film surface caused by the *trans–cis* photoisomerization of azobenzene.[7,14–18] Such a bending motion enables various actuation devices including motors,[19] inchworm walkers,[20] artificial cilia,[21] and grippers.[22]

Another type of LCEs, which does not contain photochromic functional groups, takes advantage of the nematic–isotropic (N–I) phase transition that occurs in the whole film upon exposure to heat.[5–12] The bulk effect leads to a reversible and dramatic linear contraction (30–400%). Despite such a large strain, the lack of a global bending motion significantly limits the soft robotic applications of this type of LCE. Although surface wrinkling and curling have been observed very recently in polysiloxane-based LCE/polystyrene bilayers, the need for an external heating source renders these bilayers impractical for soft robotic applications.[23]

Herein, we report a general approach to wavelength-selective, IR light-driven hinges composed of one active LCE composite layer with IR-active fillers and one passive silicone layer. IR-active fillers include single-walled carbon nanotubes (SWNTs) and near IR (NIR) dyes. Our LCE composite/silicone bilayer hinges not only show fast, reversible bending with a large strain owing to the bulk N–I LCE phase transition, but also exhibit IR wavelength selectivity by using NIR dyes as fillers. IR light better than either UV or visible light in the field of photoresponsive materials, because IR light can penetrate much deeper in most polymeric materials,[14,24] and it generally causes little damage to the material compared with UV or visible light. Such composite bilayer hinges can be used in various remote-controlled soft-robotic devices such as active origami structures that can reversibly fold and unfold, Venus flytrap-inspired grippers that can pick up delicate objects even under water, and inchworm walkers that can crawl up a hill at a 50° incline. Although we have focused on side-on LCEs synthesized from acrylate-based mesogenic monomers and silicone in this work, our approach is also applicable to other types of LCEs based on a bulk N–I phase transition and any passive elastomers.

Chemical structures of the monomers and cross-linker that were used to synthesize the side-on LCE matrix are shown in the Supporting Information, Scheme S1. We chose this particular type of LCE for two reasons: 1) it exhibits muscle-like physical properties; and 2) the N–I phase transition temperature is tunable by adjusting the ratio of two monomers.[11] The synthesis, purification, and characterization of the two mesogenic monomers were based on the literature.[11] LCE composite films were prepared using a two-stage photopolymerization process coupled with a hot-drawing technique.[25] The silicone elastomer we chose is Ecoflex, which was prepared according to the manufacturer's instructions.[2] The LCE composite/silicone bilayer films were prepared using silicone resin as an adhesive. All experimental details are available in the Supporting Information.

We and other research groups have previously reported that carbon nanotube (CNT)–LCE composite films exhibit a significant and reversible contraction upon IR irradiation.[25–28] In a SWNT–LCE composite, semiconducting SWNTs can efficiently absorb and transform IR light into thermal energy, thereby serving as nanoscale heaters uniformly embedded in the LCE matrix.[25] The absorbed

[*] R. R. Kohlmeyer, Prof. J. Chen
Department of Chemistry and Biochemistry
University of Wisconsin-Milwaukee
3210 North Cramer Street, Milwaukee, WI 53211 (USA)
E-mail: jianchen@uwm.edu

[**] This work was supported by the National Science Foundation (CMMI-0856162) and UWM Research Growth Initiative award.

Supporting information for this article is available on the WWW under http://dx.doi.org/10.1002/anie.201210232.

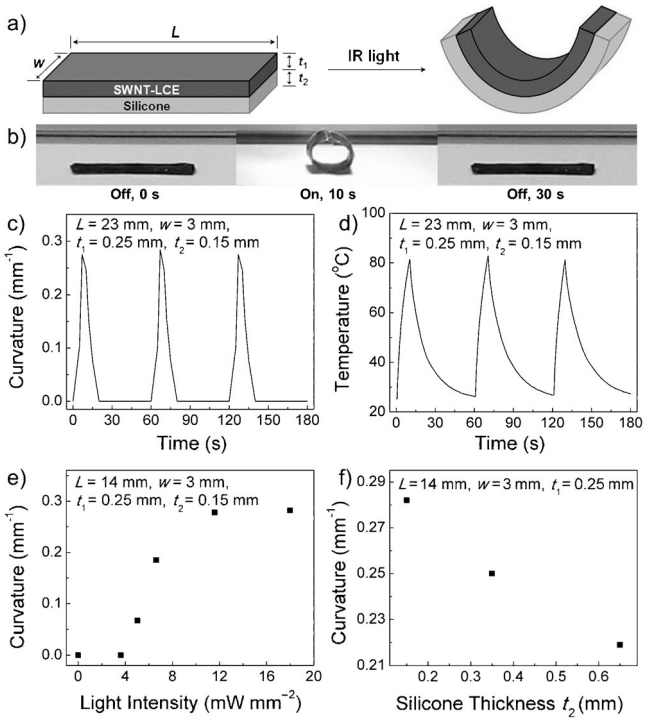

Figure 1. a) Scheme of a SWNT-LCE composite/silicone bilayer film undergoing bending toward the SWNT-LCE side upon IR irradiation, where L = length and w = width of the bilayer, t_1 = thickness of the SWNT-LCE layer, and t_2 = thickness of the silicone layer. b) Reversible bending and unbending of the SWNT–LCE/silicone bilayer film in response to continuous-wave (CW) NIR light (11.0 mW mm^{-2}). c) Curvature and d) temperature of the same bilayer film as a function of on and off cycles of CW NIR light (11.0 mW mm^{-2}). e) Curvature of the bilayer film after 10 s of IR irradiation as a function of CW NIR light intensity. f) Maximum curvature of the bilayer film upon IR irradiation as a function of silicone layer thickness when irradiated by CW NIR light (28.2 mW mm^{-2}). The SWNT loading is 0.1 wt% for all samples in Figure 1.

thermal energy, if sufficient, then induces the LCE N–I phase transition, which leads to a shape change of the nanocomposite film. Figure 1 a shows a schematic illustration of a SWNT–LCE composite/silicone bilayer film. Upon IR irradiation, the SWNT–LCE layer in the bilayer film undergoes a significant in-plane negative strain.[25] Because the SWNT–LCE layer is tightly bound to the silicone elastomer layer, in-plane contraction is impossible and instead in-plane negative strain bends the underlying silicone elastomer layer (Figure 1 a). IR-induced bending actuation of the bilayer film is large, fast, and reversible (Figure 1 b,c; Supporting Information, Video S1), which makes the bilayer film an excellent remote-controlled hinge for soft robotics. The temperature of a 0.1 wt% SWNT–LCE/silicone bilayer film reaches over 80 °C soon after the IR light is turned on (Figure 1 d), which is well above the N–I phase transition temperature (64.6 °C). This confirms the role of SWNTs as IR-absorbing nanoscale heaters. IR-induced bending actuation can be controlled by adjusting the IR light intensity and silicone layer thickness, among others. The IR-induced curvature of a bilayer film increases with higher IR light intensity around the N–I phase transition temperature (Figure 1 e) and thinner silicone-layer thickness (Figure 1 f).

The 0.1 wt% SWNT–LCE/silicone bilayer film starts to bend as the IR light intensity exceeds 4 mW mm^{-2} (Figure 1 e). For instance, the curvature and temperature of the bilayer film reach 0.07 mm^{-1} and approximately 56 °C, respectively, when the IR light intensity is 5.0 mW mm^{-2}. The modest bending of the bilayer film at lower IR light intensity (e.g., 5.0 mW mm^{-2}) most likely arises from the small negative strain in the heated LCE monolayer below the N–I phase transition temperature.[11] The sharpest rise in curvature occurs, as expected, when the bilayer film temperature (approximately 64–65 °C) reaches the N–I phase transition temperature upon 6.6 mW mm^{-2} of IR irradiation. The curvature and temperature of the bilayer film further increase to 0.28 mm^{-1} and approximately 89 °C, respectively, as the IR light intensity reaches 11.6 mW mm^{-2}. Little change in curvature is observed once the IR light intensity exceeds 12 mW mm^{-2} (Figure 1 e) despite that the temperature of the bilayer film continues to increase (e.g., $T \approx 136$ °C; light intensity = 18.0 mW mm^{-2}). This indicates that the IR-induced bending mainly originates from the N–I phase transition instead of the difference of coefficient of thermal expansion between the CNT–LCE layer and silicone layer. This bending mechanism is fundamentally different from that of an azobenzene LCE/polyethylene laminated film, where the enhanced curling is attributed to the difference in the thermal expansion coefficients between the two layers.[20]

Active origami structures can fold from a flat sheet into complex 3D shapes upon exposure to an external stimulus such as heat. Although shape-memory polymers can be designed to fold into 3D shapes such as a box, the folding is normally irreversible without applying an external mechanical force.[29–31] Our bilayer hinges can be used in conjunction with passive materials such as polycarbonate (PC) films to assemble various foldable structures that can repeatedly undergo reversible IR-induced folding and unfolding (Figure 2 a–c; Videos S2, S3). In particular, Figure 2 c shows a foldable structure inspired by a Venus flytrap, which can open and close repeatedly in response to IR light (Video S3). We designed our grippers based on such a Venus flytrap-inspired structure for its simplicity and versatility. The gripper consists of two curved PC films serving as arms that are connected by a number of bilayer hinges (Figure 2 d), which can be used to pick up and place objects of various shapes such as a toy figure (Figure S1; Video S4) and a safety pin, whose metal wire diameter is less than 1 mm (Figure 2 e; Video S5). The closing and opening of the arms of the gripper are controlled by turning on and off the IR light. By increasing the length and strength of the PC arms (Figure 2 f), the gripper can overcome the viscosity of water and pick up a plastic dumbbell from the bottom of a beaker of water (Figure 2 g; Video S6). Both the shape and size of the PC arm could be further modified to better conform to the shape of an object (e.g., a ball). The strength of a gripper could be enhanced, for instance, by increasing the number of hinges used in the gripper.

Polymer-based inchworm walker devices have attracted significant interest in recent years.[20,32–34] These devices, which

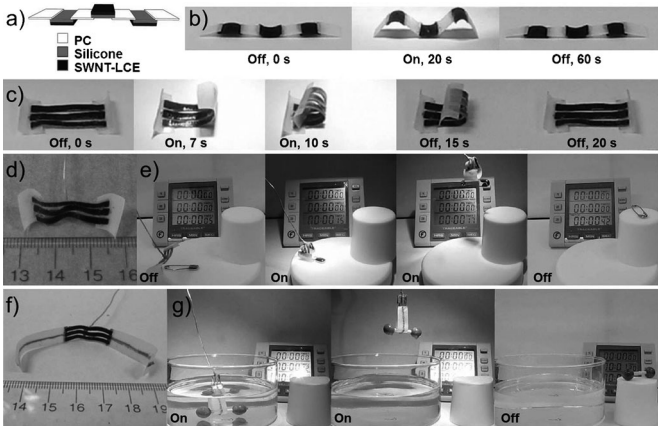

Figure 2. a) Scheme of an origami structure of four polycarbonate (PC) films ($L = 5$ mm; $w = 5$ mm; $t = 0.1$ mm) that are adhesively connected by three SWNT–LCE/silicone bilayer hinges ($L = 5$ mm; $w = 5$ mm; $t_1 = 0.25$ mm; $t_2 = 0.15$ mm). b) Reversible folding and unfolding of the origami structure in response to CW NIR light (11.0 mW mm^{-2}). c) Reversible closing and opening of a Venus flytrap-inspired gripper in response to CW NIR light (28.2 mW mm^{-2}). The structure has two curved PC films ($L = 15$ mm; $w = 10$ mm; $t = 0.1$ mm) that are connected by three SWNT–LCE/silicone bilayer hinges ($L = 23$ mm; $w = 2$ mm; $t_1 = 0.25$ mm; $t_2 = 0.15$ mm). d) A Venus flytrap-inspired short gripper, which has two curved PC films serving as arms, connected by three SWNT–LCE/silicone bilayer hinges of the same size as in Figure 2c. The center of the structure is adhesively bonded to a thin metal wire handle. e) Using the same short gripper from Figure 2d to pick up a safety pin and place it on a platform. The arms of the gripper are controlled by CW NIR light (28.2 mW mm^{-2}). f) A longer gripper having 25 mm long PC arms adhesively reinforced by thin metal wires. g) Using the long gripper from Figure 2f to pick up a plastic dumbbell from under water and place it on a platform under the same IR conditions as in Figure 2e. The SWNT loading is 0.1 wt% for all samples in Figure 2.

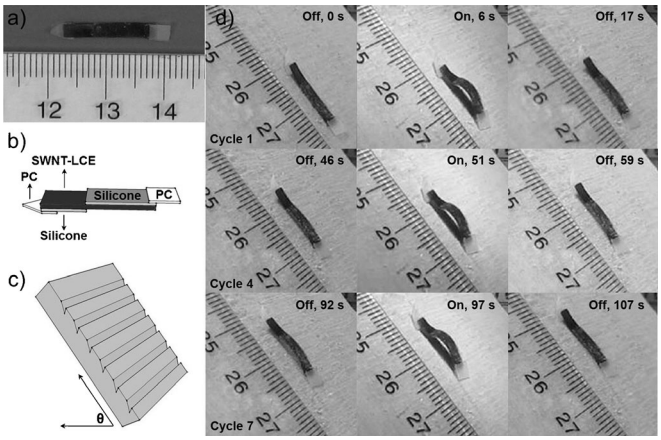

Figure 3. a) Photograph and b) scheme of an inchworm walker device consisting of an asymmetric SWNT–LCE/silicone bilayer film ($L_{\text{SWNT-LCE}} = 15$ mm; $w_{\text{SWNT-LCE}} = 3$ mm; $t_{\text{SWNT-LCE}} = 0.25$ mm; $L_{\text{silicone top}} = 9$ mm; $w_{\text{silicone top}} = 3$ mm; $t_{\text{silicone top}} = 0.15$ mm; $L_{\text{silicone bottom}} = 6$ mm; $w_{\text{silicone bottom}} = 3$ mm; $t_{\text{silicone bottom}} = 0.15$ mm) and two PC films with different shapes ($L_{\text{top}} = 4$ mm; $w_{\text{top}} = 3$ mm; $t_{\text{top}} = 0.1$ mm; $L_{\text{bottom 1}} = 3$ mm; $L_{\text{bottom 2}} = 2$ mm; $L_{\text{bottom 3}} = 3$ mm; $t_{\text{bottom}} = 0.1$ mm). c) Scheme of a ratcheted wood substrate. d) The inchworm walker crawling up the wood substrate at a 50° incline in response to on and off cycles of CW NIR light (28.2 mW mm^{-2}). The SWNT loading is 0.1 wt% for all samples in Figure 3.

can move on flat substrates, include a chemically responsive polymer gel,[32] a UV/visible light-responsive azobenzene LCE/polyethylene laminated film,[20] a humidity-responsive polyelectrolyte multilayer film,[33] and an electroresponsive graphene/polydiacetylene bilayer film.[34] In contrast to previous walking devices, we show herein an IR light-driven inchworm walker that can crawl up a hill at a 50° incline. The inchworm walker is comprised of an asymmetric SWNT-LCE/silicone bilayer film and two PC films with different shapes (Figure 3a,b). The asymmetric design of the bilayer film allows its front part and back part to bend outward and inward, respectively, upon IR irradiation. In the beginning of each actuation cycle, the center of the IR light is pointed at the front of the device, causing the front part of the bilayer film to bend outward, which forms the stationary point on the substrate. Next, the center of the IR light moves to the center of the device, causing the back part of the bilayer film to bend inward, so that the second half of the device slides forward. Finally, the IR light is turned off, which allows the whole bilayer film to unbend and the first half of the device to slide forward (Figure 3d; Video S7). The ratcheted substrate and the rectangular-shaped PC film at the end of the walker prevent the device from sliding backward (Figure 3c,d). This device can also walk directionally on a flat, smooth wood substrate in response to on/off cycles of IR light. This observation clearly suggests that the directional movement of the device is mainly enabled by the directional movement of IR light from the front to the center of the device and corresponding directional IR actuation, not by the ratcheted substrate. The walking velocity of our IR light-driven device on the tilting substrate at the 50° incline is approximately 0.1 mm s^{-1}, which is similar to that (approximately 0.15 mm s^{-1}) of the UV/visible light-responsive azobenzene LCE/polyethylene laminated film device on a flat surface,[20] but over thirty times faster than that (approximately 0.003 mm s^{-1}) of the chemically responsive polymer-gel device on a flat surface.[32]

IR wavelength-selective irradiation is highly desirable because it could ultimately enable precise and independent control of each individual actuator (e.g., a hinge) using a predetermined specific IR laser wavelength within a single soft-robotic system. Our approach to IR wavelength-selective hinges involves the use of commercial proprietary NIR dyes as fillers. Dye 1002, whose structure is shown in Scheme S2, has an NIR absorption peak maximum around 1007 nm in solution, but the same peak broadens dramatically and is red-shifted by 25 nm to 1032 nm in a 0.2 wt% Dye 1002-LCE composite film (Figure 4a). The temperature of a 0.2 wt% Dye 1002-LCE/silicone bilayer film increases to 69 °C upon laser irradiation at 980 nm with an intensity of 5.7 mW mm^{-2} (Figure 4b), which exceeds the N–I phase transition temperature (61.4 °C) of the 0.2 wt% Dye 1002-LCE composite layer and triggers the bending of the bilayer film (Figure 4c). In contrast, the temperature of the same bilayer film only reaches 29 °C when irradiated by the 1342 nm laser at the same intensity (Figure 4b) and therefore no bending occurs (Figure 4d). Tunability of the IR wavelength is possible by

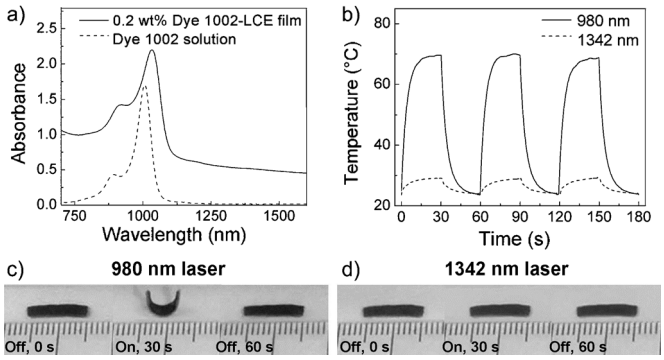

Figure 4. a) Vis-NIR absorption spectra of a Dye 1002 chloroform solution and 0.2 wt% Dye 1002-LCE composite film. b) Temperature profiles of a 0.2 wt% Dye 1002-LCE/silicone bilayer film ($L = 11$ mm; $w = 3$ mm; $t_1 = 0.17$ mm; $t_2 = 0.24$ mm) irradiated by IR lasers with two different wavelengths at an intensity of 5.7 mW mm^{-2}. c) Bending occurs when the 0.2 wt% Dye 1002-LCE/silicone bilayer film is irradiated by a 980 nm laser (5.7 mW mm^{-2}). d) No bending is observed when the same bilayer film is irradiated by a 1342 nm laser at the same intensity.

choosing different NIR dyes and a matching IR laser wavelength. Although the use of a different NIR dye (Lumogen IR 788) in a liquid crystal polymer has been reported very recently, no IR wavelength-selective irradiation has been demonstrated.[35]

In summary, we have developed a general approach to wavelength-selective, IR light-driven LCE composite-based bilayer hinges that show fast, reversible bending with a large strain originating from the bulk LCE N–I phase transition. Such composite bilayer hinges can power various remote-controlled soft robotic devices, including active origami structures, Venus flytrap-inspired grippers, and climbing inchworm walkers. NIR dyes are promising fillers for tunable IR wavelength-selective actuation of shape-changing polymers and programming of shape-memory polymers.

Received: December 22, 2012
Revised: February 3, 2012
Published online: March 8, 2013

Keywords: actuators · liquid crystals · nanotubes · polymers · soft robotics

[1] D. Trivedi, C. D. Rahn, W. M. Kier, I. D. Walker, *Appl. Bionics Biomech.* **2008**, *5*, 99 – 117.
[2] F. Ilievski, A. D. Mazzeo, R. F. Shepherd, X. Chen, G. M. Whitesides, *Angew. Chem.* **2011**, *123*, 1930 – 1935; *Angew. Chem. Int. Ed.* **2011**, *50*, 1890 – 1895.
[3] R. F. Shepherd, F. Ilievski, W. Choi, S. A. Morin, A. A. Stokes, A. D. Mazzeo, X. Chen, M. Wang, G. M. Whitesides, *Proc. Natl. Acad. Sci. USA* **2011**, *108*, 20400 – 20403.
[4] S. A. Morin, R. F. Shepherd, S. Wai Kwok, A. A. Stokes, A. Nemiroski, G. M. Whitesides, *Science* **2012**, *337*, 828 – 832.
[5] H. Finkelmann, H. J. Kock, G. Rehage, *Makromol. Chem. Rapid Commun.* **1981**, *2*, 317 – 322.
[6] M. Warner, E. M. Terentjev, *Liquid Crystal Elastomers*, Oxford University Press, Oxford, **2007**.
[7] T. Ikeda, J. Mamiya, Y. Yu, *Angew. Chem.* **2007**, *119*, 512 – 535; *Angew. Chem. Int. Ed.* **2007**, *46*, 506 – 528.
[8] C. Ohm, M. Brehmer, R. Zentel, *Adv. Mater.* **2010**, *22*, 3366 – 3387.
[9] *Cross-linked Liquid Crystalline Systems: From Rigid Polymer Networks to Elastomers* (Eds.: D. Broer, G. Crawford, S. Žumer), CRC, Boca Raton, FL, **2011**.
[10] H. Yang, G. Ye, X. Wang, P. Keller, *Soft Matter* **2011**, *7*, 815 – 823.
[11] D. L. Thomsen III, P. Keller, J. Naciri, R. Pink, H. Jeon, D. Shenoy, B. R. Ratna, *Macromolecules* **2001**, *34*, 5868 – 5875.
[12] J. Naciri, A. Srinivasan, H. Jeon, N. Nikolov, P. Keller, B. R. Ratna, *Macromolecules* **2003**, *36*, 8499 – 8505.
[13] M. Behl, J. Zotzmann, A. Lendlein, *Adv. Polym. Sci.* **2010**, *226*, 1 – 40.
[14] M. Kondo, Y. Yu, T. Ikeda, *Angew. Chem.* **2006**, *118*, 1406 – 1410; *Angew. Chem. Int. Ed.* **2006**, *45*, 1378 – 1382.
[15] S. Serak, N. Tabiryan, R. Vergara, T. J. White, R. A. Vaia, T. J. Bunning, *Soft Matter* **2010**, *6*, 779 – 783.
[16] K. M. Lee, M. L. Smith, H. Koerner, N. Tabiryan, R. A. Vaia, T. J. Bunning, T. J. White, *Adv. Funct. Mater.* **2011**, *21*, 2913 – 2918.
[17] W. Wu, L. Yao, T. Yang, R. Yin, F. Li, Y. Yu, *J. Am. Chem. Soc.* **2011**, *133*, 15810 – 15813.
[18] W. Wang, X. Sun, W. Wu, H. Peng, Y. Yu, *Angew. Chem.* **2012**, *124*, 4722 – 4725; *Angew. Chem. Int. Ed.* **2012**, *51*, 4644 – 4647.
[19] M. Yamada, M. Kondo, J. Mamiya, Y. Yu, M. Kinoshita, C. J. Barrett, T. Ikeda, *Angew. Chem.* **2008**, *120*, 5064 – 5066; *Angew. Chem. Int. Ed.* **2008**, *47*, 4986 – 4988.
[20] M. Yamada, M. Kondo, R. Miyasato, Y. Naka, J. Mamiya, M. Kinoshita, A. Shishido, Y. Yu, C. J. Barrett, T. Ikeda, *J. Mater. Chem.* **2009**, *19*, 60 – 62.
[21] C. L. van Oosten, C. W. M. Bastiaansen, D. J. Broer, *Nat. Mater.* **2009**, *8*, 677 – 682.
[22] F. Cheng, R. Yin, Y. Zhang, C.-C. Yen, Y. Yu, *Soft Matter* **2010**, *6*, 3447 – 3449.
[23] A. Agrawal, P. Luchette, P. Palffy-Muhoray, S. Lisa Biswal, W. G. Chapman, R. Verduzco, *Soft Matter* **2012**, *8*, 7138 – 7142.
[24] R. R. Kohlmeyer, M. Lor, J. Chen, *Nano Lett.* **2012**, *12*, 2757 – 2762.
[25] L. Yang, K. Setyowati, A. Li, S. Gong, J. Chen, *Adv. Mater.* **2008**, *20*, 2271 – 2275.
[26] Y. Ji, Y. Y. Huang, R. Rungsawang, E. M. Terentjev, *Adv. Mater.* **2010**, *22*, 3436 – 3440.
[27] C. Li, Y. Liu, C.-W. Lo, H. Jiang, *Soft Matter* **2011**, *7*, 7511 – 7516.
[28] J. E. Marshall, Y. Ji, N. Torras, K. Zinoviev, E. M. Terentjev, *Soft Matter* **2012**, *8*, 1570 – 1574.
[29] M. Behl, M. Y. Razzaq, A. Lendlein, *Adv. Mater.* **2010**, *22*, 3388 – 3410.
[30] Y. Liu, J. K. Boyles, J. Genzer, M. D. Dickey, *Soft Matter* **2012**, *8*, 1764 – 1769.
[31] J. Ryu, M. D'Amato, X. Cui, K. N. Long, H. J. Qi, M. L. Dunn, *Appl. Phys. Lett.* **2012**, *100*, 161908.
[32] S. Maeda, Y. Hara, T. Sakai, R. Yoshida, S. Hashimoto, *Adv. Mater.* **2007**, *19*, 3480 – 3484.
[33] Y. Ma, Y. Zhang, B. Wu, W. Sun, Z. Li, J. Sun, *Angew. Chem.* **2011**, *123*, 6378 – 6381; *Angew. Chem. Int. Ed.* **2011**, *50*, 6254 – 6257.
[34] J. Liang, L. Huang, N. Li, Y. Huang, Y. Wu, S. Fang, J. Oh, M. Kozlov, Y. Ma, F. Li, R. Baughman, Y. Chen, *ACS Nano* **2012**, *6*, 4508 – 4519.
[35] L. T. de Haan, C. Sánchez-Somolinos, C. M. W. Bastiaansen, A. P. H. J. Schenning, D. J. Broer, *Angew. Chem.* **2012**, *124*, 12637 – 12640; *Angew. Chem. Int. Ed.* **2012**, *51*, 12469 – 12472.